CHAPTER VI

THE FORMATION, NUMBERS AND RADIO LUMINOSITIES OF GIANT RADIO GALAXIES

6.1 INTRODUCTION

Until the discovery of the giant radio galaxies 3C236 and DA240 by Willis, Strom and Wilson (1974), the sizes of double radio sources were known to be within a megaparsec. Even today this is largely true, with most sources having sizes between 200 - 500 kpc, but existence of a small percentage (<5%) on the megaparsec scale has been clearly established (Miley, 1980; Saripalli et al., 1986). Of the several hundred radio galaxies mapped so far, the total number of known GRGs is less than 20. The rarity of these objects poses questions concerning their formation: (a) could the GRGs be associated with nuclear activity of modest intrinsic power but of extremely long duration? or, (b) are they produced by powerful engines over relatively normal time scales? These basic questions pertaining to an extreme type of phenomenon have received rather little attention in the literature. In the previous chapters, statistical, comparative studies of GRGs have been presented which have indicated the important role of the central engine in the formation of their exceptional sizes.

In this chapter we investigate the conditions for formation of GRGs adopting a theoretical approach. We argue in favour of their formation via powerful engines over normal time scales, employing a generalized version of the recent model for radio beam propagation, of Gopal-krishna and Wiita (1987; GW).

In this model, a radio beam first propagates through the gaseous halo of the parent elliptical galaxy, which is nearly isothermal, and has a density profile roughly given by $n \propto r^{-1.5}$ (e.g., Forman,Jones and Tucker, 1985; see also Strom and Jägers, 1988). Then the beam enters an even hotter but much less dense intergalactic medium (IGM), after crossing a pressure-matched halo-IGM interface. The properties of the IGM have recently been derived from the analysis of the observed diffuse (3-200 KeV) X-ray background (e.g., Guilbert and Fabian, 1986; Barcons, 1987). Since both density and temperature of the IGM rise steeply with cosmological redshift, the halo/IGM interface would occur closer to the galactic nucleus at earlier epochs. The advance of the relativistic beam is considered to be halted by the deceleration of the head of the beam to the sound velocity in the ambient medium, or by the cessation of the nuclear activity.

The extremities of classical double radio sources, usually associated with relatively isolated elliptical galaxies, are frequently marked by hot spots whose separation, 2D, has a median value of 300 - 400 kpc at small redshifts. Recently, it has been established that the median size decreases with redshift as $(1+z)^{-\sigma}$, where σ is estimated to be about 2 or 3 (Kapahi, 1985; Eales, 1985; Gopal-Krishna et al., 1986; Oort et al., 1987a,b; Singal, 1988). The simple analytical models for beam propagation through the halo and IGM presented in GW was able to predict the exponent $\sigma \simeq 3$ as confirmed by Oort et al., (1987b) and Singal(1988). The prediction of this analytical model has also been confirmed by numerical simulations of the jets using a boundary-following code (Rosen and Wiita, 1988; hereafter referred to as RW).

Both GW and RW considered typical classical double sources, and the possibility of relativistic motion of the head of the beam was not taken into account. However, when considering extremely energetic beams, relativistic motion of the head is to be expected, at least over the early part of the source's life. On the other hand, during the later stages when the source has grown to very large volumes, the magnetic energy density in the radio lobes is expected to fall below the energy density of the Microwave Background Photons. Under such conditions, the radio-emitting relativistic electrons would preferentially loose energy through inverse Compton collisions with the background photons, generating X-rays and thereby supressing the radio output (see Gopal-Krishna,Wiita and Saripalli, 1988). This reduced radio efficicency (RRE) would set in at a fairly early stage in sources energised by low-power beams, particularly, at high redshifts where the microwave background is stronger. With the concept of RRE we are able to account for the observed low powers of GRGs which seem to defy the known positive correlation ($D \propto P^{0.3}$) between the radio power and linear size (Gavazzi and Perola, 1978; Ekers et al., 1981; Kapahi, 1986; Machalski and Condon, 1985; Oort et al., 1987a; Alexander and Leahy, 1987; Singal, 1988).

6.2 BEAM DYNAMICS IN THE RELATIVISTIC LIMIT

We assume the beam fluid to have a relativistic equation of state and a relativistic bulk velocity. The beam opening angle, within the halo, θ, is assumed to remain constant as in GW and in Model A of Scheuer (1974). The opening angle, θ is observed to be smaller for sources with higher powers (Bridle, 1986). We have incorporated this effect, and describe the procedure adopted, below. When we make the additional assumption, that the beam power, L_b, is predominently kinetic, we get (e.g., O'Dea, 1985).

$$L_b = \frac{\pi\theta^2 D^2}{4} \rho_b c^2 \gamma_b (\gamma_b - 1) \beta_b c \qquad \ldots(6.1)$$

where D is the length of the beam at a given time, and ρ_b, $c\beta_b$ and γ_b are the density, bulk velocity and bulk Lorentz factor of the beam, respectively. Following Blandford and Rees (1974) we assume that the beam flow is strongly decelerated and thermalised at a termination shock, typically marked by a hotspot, which is advancing with a velocity $c\beta_h$ in pressure balance with the external medium, as in Scheuer (1974). Transforming to the shock frame, where the beam velocity is $c\beta'_b$, we obtain

$$\frac{\pi}{4}\theta^2 D^2 \rho_b (\gamma'_b \beta'_b c)^2 = \frac{\pi}{4}\theta^2 D^2 \rho_{ext} (\gamma_h \beta_h c)^2, \qquad \ldots(6.2)$$

taking $\gamma_b >> 1$ and ρ_{ext} to be the ambient density which is assumed to be a function of D inside the halo and constant beyond, in the IGM. Using the relations, $\beta'_b = (\beta_b - \beta_h)/(1-\beta_b\beta_h)$ and $\gamma'_b = \gamma_b\gamma_h(1-\beta_b\beta_h)$ and noting that $\beta_b \simeq 1$, we have the result:

$$\frac{\beta_h}{1-\beta_h} = \frac{1}{D}\left\{\frac{4L_b}{\pi c^3\theta^2\rho_{ext}(D)}\right\}^{1/2}. \qquad \ldots(6.3)$$

Following Forman et al. (1985) and GW, within the halo we take

$$\rho_{ext}(D) = \frac{n_o m_H \mu}{[1+(D/a)^2]^{\delta}} \qquad \ldots(6.4)$$

with n_o, the central density, m_H, the mass of a hydrogen atom, μ, the mean molecular weight, a, the core radius of the gaseous halo and δ estimated to be 0.75 ± 0.15. Throughout this work, we use the best average values of $n_o = 10^4 m^{-3}$, a = 2 kpc, $\mu = 0.6$ and $\delta = 0.75$; the temperature of the halo is taken to be constant, with kT = 1 KeV (Forman et al., 1985). As argued in GW (see also, Rana and Wilkinson, 1987), it is assumed that the halo properties have not evolved significantly out to a redshift of one.

Using Eq.(6.4) and Eq.(6.3), we obtain

$$V(D) = \frac{Xc[1+(D/a)^2]^{\delta/2}}{D+X[1+(D/a)^2]^{\delta/2}}, \qquad \ldots(6.5)$$

where $X = \left(\frac{4L_b}{\pi c^3\theta^2 n_o m_H \mu}\right)^{1/2}$ and V is the velocity of advance of the head of the beam.

In order to incorporate the known dependence of θ on P into our model, we need to estimate the dependence of θ upon the beam power, L_b. This requires transforming the P-θ diagram shown in Fig.2 of Bridle (1986) into an L_b-θ relation, which, in turn, needs an estimate of the mean radio efficiency (see below) for sources of different powers. These estimates were obtained by a single iteration, starting with the assumption of a constant initial opening angle (θ=0.04 radian; see GW) for all sources and predicting the time-evolution of their radio output as described below. It is found that at a small redshift of 0.1, characteristic of the sources plotted in Fig.2 of Bridle (1986), the typical radio luminosity (emitted at its mean age, $t_N/2$) is $\sim$30% of the initial luminosity, P_o, for powerful sources (P $\approx 10^{28}$ WHz^{-1} at 1 GHz) but only $\sim$3% for moderately powerful sources with P $\approx 10^{25}$ WHz^{-1}. This, combined with the P-θ diagram of Bridle (1986), leads to an approximately linear relation between L_b and θ:

$$\theta\,(\text{in radians}) = 0.02 + 0.03\left[39 - \mathrm{Log}\{0.2\, L_b\,(\text{in watts})\}\right]$$

For the most powerful sources, the P-θ diagram shows that θ approaches a minimum value of $\sim$0.02 radian, which we adopt for the above relation as well. Expressing D in units of kpc (X is also in kpc) and solving Eq.(6.5), we obtain for $(D/a)^2 \gg 1$,

$$t = \frac{1}{Xc}\left\{\frac{a^{\delta}}{2-\delta}\cdot D^{2-\delta} + XD\right\}. \qquad \ldots(6.6)$$

Within the halo, it is not possible to solve for D in closed form in terms of t. As expected, the above two equations reduce to Eq(6.5) and Eq(6.6) of GW, in the limit $\beta_h \ll 1$. The above derivation holds for the beam propagation while $D < R_h$, the halo/IGM interface defined by the pressure matching condition. We then find $R_h(z) = R_h(z=0)\,(1+z)^{-5/2\delta}$ with $R_h\,(z=0) = 171$ kpc (GW).

In order to investigate the beam propagation outside the halo ($D > R_h$) analytically, we have to consider two extreme possibilities designated Model A and Model B in GW and RW. It should be noted that the numerical simulations presented in RW suggest that the true behaviour of the beam lies almost midway between these two models.

In Model A, the opening angle, θ , of the beam is taken to remain constant upon crossing the interface, implying that β_h rises abruptly owing to the sudden drop in the ambient density. Following Guilbert and Fabian (1986) $n_{IGM}(z) = n_{IGM}(0)\,(1+z)^3$, with $n_{IGM}(0) = 7.10^{-1}\,m^{-3}$, and $T_{IGM}(z) = T_{IGM}(0)(1+z)^2$ with $kT_{IGM}(0) = 1\ 8$ KeV. In this model, using the same assumption for the ram-pressure balance (GW), we obtain for the generalized case,

$$V(D) = \frac{cX'}{D+X'}, \quad \text{with } X' = X\left\{\frac{n_o}{n_{IGM}(0)(1+z)^3}\right\}^{1/2} \qquad ...(6.7)$$

and,

$$D(t) = \left\{X'^2 + 2X'ct + \left[R_h^2(z) - \frac{2a^\delta}{2-\delta}\,R_h^{2-\delta}(z)\left\{\frac{n_o}{n_{IGM}(0)(1+z)^3}\right\}\right]\right\}^{1/2} - X' \qquad (6.8)$$

These equations reduce to Eq(8) and Eq(9) of GW for $\beta_h \ll 1$.

For Model B, where β_h is taken to be continuous across the halo/IGM interface, the beam opening angle abruptly increases to a larger value, θ_{IGM}, given by (GW, Eq.10)

$$\theta_{IGM} = \theta\{\frac{a}{R_h(z)}\}^{\delta} [\frac{n_o}{n_{IGM}(0)(1+z)^3}]^{1/2} \quad ...(6.9)$$

In this case, we find,

$$V(D) = \frac{cX''}{D+X''}, \text{ with } X'' = X(\theta/\theta_{IGM})\{n_o/[n_{IGM}(0)(1+z)^3]\}^{1/2}; \quad ...(6.10)$$

$$D(t) = \{X''^2+2X''[ct + \frac{a^{\delta}R_h(z)^{2-\delta}}{X}(\frac{1}{2} - \frac{1}{2-\delta})]\}^{1/2} - X'' \quad ...(6.11)$$

Once again, these reduce to Eq(11) and Eq(12) of GW for $\beta_h \ll 1$.

The abrupt flaring of the jet in Model B has apparently been observed in some well resolved radio jets (see Sect.3.2 of GW) as well as in both the boundary following simulations (RW) and preliminary full 2-dimensional hydrodynamical simulations (Wiita, Rosen and Norman, in preparation). These simulations also reveal the acceleration of the beam head at the interface predicted by Model A.

6.3 THE TIME EVOLUTION OF THE RADIO OUTPUT AND THE LINEAR SIZE

For comparison with observations we express the results in terms of a monochromatic radio power, P , which is assumed to scale closely with the bolometric radio power, L_R, and is thus evaluated at = 1 GHz (roughly at the logarithmic centre of the radio band), by assuming a typical spectral index of $\alpha = -0.8$. Here L_R is $= P \int d\nu$, evaluated between 10^7 and 10^{11} Hz; hereafter we will drop the subscript ν from P_ν.

Two simplifying assumptions concerning extended radio sources, that are customarily made in the literature, are : (i) the applicability of the minimum energy condition, implying that the relativistic electrons have 4/3 times the energy density of the magnetic field; and (ii) the bolometric radio emission, L_R, is a fairly fixed fraction of the total beam power, $2L_b$, and that the beam power is constant in time (see, e.g.,Begelman, Blandford and Rees, 1984). The constancy of L_b over the source lifetime is a simplifying assumption. It has received some support from the recently reported correlation between the nuclear emission in the [OIII] line indicative of the current beam power, and the time-averaged beam power, estimated by dividing the minimum energy content of the radio lobes by their spectral ages (Rawlings and Saunders, 1988). In this work we essentially retain these assumptions with the modification that while L_R is initially equal to a constant fraction, ϵ, of $2L_b$, with ϵ typically 0.1 (e.g., Gopal-Krishna and Saripalli, 1984a; Dreher, 1984; Saripalli and Gopal-Krishna, 1985) we allow for a gradual reduction of the radio efficiency as the internal magnetic energy density of the lobes, u_B, approaches the energy density of the microwave background, $u_{ph}(z) = 4.8.10^{-14} (1+z)^4$ Joules.m^{-3} (Lang, 1978). This concept of 'reduced radio efficiency' (RRE) is particularly relevant in the case of highly extended double radio sources since a large fraction of their radio emission originates from the lobes (e.g., Jägers, 1986; Leahy and Williams, 1984) whose ${}_B$ is appreciably lower than that in the hot spots and falls below u_{ph} sooner. Earlier, Rees and Setti, (1968), considered within the framework of the plasmon model,the possibility that radio lobes of weak double sources might be 'snuffed out' due to increased inverse Compton losses at high redshifts. Applying this idea to an actually observed sample of nearby sources, Scheuer (1977) argues that this snuffing out is unlikely to account for the much slower cosmological evolution of weaker radio sources, inferred from the radio source counts (Longair, 1966). Although the inverse Compton losses may not be severe enough to effectively extinguish the sources even at high redshifts, as argued by Eales (1985), they will certainly reduce the radio output. Here, the resulting RRE is quantitatively estimated and applied within the framework of the relativistic beam model.

Due to the large dispersion in the properties of radio sources it is not possible to give a precise derivation of the extent of RRE. Nevertheless, taking into account the known structures of large double sources and general physical constraints we have arrived at the following estimate of the effect. We assume that the radio output as a function of the time, can be written as,

$$L_R(t) = \varepsilon'(t)L_R(0) = \varepsilon'(t)\epsilon 2L_b \qquad \text{...(6.12a)}$$

with no inverse Compton losses present at $t = 0$. Once they set in we assume $L_R(0) = L_R(t)+L_X(t)$, with L_X the X-ray emission from upscattered microwave photons, so that

$$\varepsilon'(t) = L_R(t)/[L_R(t) + L_X(t)] = [1+(u_{ph}(z)/\langle u_B\rangle)]^{-1} \qquad (6.12b)$$

with $\langle u_B\rangle$ the average magnetic energy density in the radio source.

In general we can set $\langle u_B\rangle = \eta\, u_{B,h}$, with $u_{B,h}$ the magnetic energy density in the hot spot(Table 3.1.1a, Chapter III), which is related to the total energy density in the hot spot, u_h, through the assumed minimum energy argument by $u_{B,h} = (3/7)u_h$. But the ram-pressure confinement of the hotspot yields $\rho_{ext}V_h^2 = (1/3)u_h$, so that

$$\langle u_B\rangle = (9/7)\eta\rho_{ext}\, V_h^2 \qquad \ldots(6.12c)$$

with V_h given by $c\beta_h$ from equation (6.5) or (6.8) or (6.10). An examination of many large and giant radio sources suggests that the magnetic fields in their lobes, which account for most of the radio emission, are typically a few times weaker than in their hot spots. Accordingly, we have adopted $\eta = 0.1$ for our present numerical work.

However, $\langle u_B\rangle$ cannot be allowed to fall below the limit set by the static confinement of the lobe due to the thermal pressure of the external medium, at which point the expansion of the lobe will be halted. This implies,

$$\langle u_B\rangle_{min} = \frac{3}{7}\langle u\rangle_{min} = \frac{3}{7}u_{ext} \simeq \frac{9}{14}\,p_{ext} \qquad \ldots(6.12d)$$

with $p_{ext}=n_{ext}kT_{ext}$ and subscript 'ext' takes on the values 'halo' and 'IGM'. By inserting the larger of (6.12c) and (6.12d) into equation (6.12b), an estimate for the total radio luminosity, (6.12a), is obtained.

As discussed in GW the observed expansion of a double source will be halted (the 'growth freeze') either when V_h decreases to $c_s(z)$, the ambient sound velocity, or when the central engine turns off after a lifetime, t_N. But, in view of RRE and the finite sensitivity of the radio observations to the total flux and surface brightness, we must also introduce an additional constraint. The largest among sensitive surveys made for discovering GRGs is the one carried out using the 6C synthesis array at 151 MHz (e.g., Baldwin et al., 1985, and references therein). For the purpose of detecting giant radio sources, the 6C survey appears to be confusion-limited below a flux density limit of ~ 5 Jy at 151 MHz (Saunders, Baldwin and Warner, 1987), corresponding to S_{lim} = 1 Jy at 1GHz (the frequency to which all our estimates are referred), assuming a spectral index $\alpha = 0.8$ ($S_\nu \propto \nu^{-\alpha}$).

6.4 RESULTS

Here, we present results, incorporating the beam power dependence of the opening angle, θ and the model for the dependence of the radio emitting efficiency on power. As will be seen below, the model yields a good match to the observed total number of GRGs at small (z<0.1) redshifts. For this we have used the radio luminosity function at different z as derived by Peacock (1987).

The results are presented in the form of Figures 6.1 and 6.2, and Tables 6.1, 6.2. The time evolution D (length of the beam), of V_h (velocity of advance of the hotspot), P (monochromatic radio power at 1 GHz), S (the total flux density at 1 GHz) have been computed for total beam power ($2L_b$) in the range 10^{32}W to 10^{40}W, and redshifts in the range 0.05 to 0.65 at intervals of 0.1. Fig.6.1. shows the L_b-D plot for a few representative ages of the source, equal to 10^6 the time scales of 10^6 yr, 10^7 yr, and the assumed nuclear lifetimes $t_N=10^8$ yr and 3.10^8 yr for three redshifts of 0.05, 0.15 and 0.35 (see GW; Stockton and Mackenty, 1987; Hutchings,1988). The onset of various constraints (see Section 6.3) in the course of the evolution of the radio sources have been marked in the (L_b-D) diagrams for each redshift. The points (function of L_b) at which the beam head becomes subsonic or S_{1GHz} = 1 Jy (detection limit) are also shown together with the estimated location of the parent galaxy's halo and the minimum half size for a GRG (D = 750 kpc).

It can be seen that for a fixed redshift a given size is attained at earlier times, for increasing beam powers. Also the various constraints become operative at larger values of D. The discontinuity in the velocity of advance of the hotspot as the beam emerges out of the galaxy halo (Model A) is clearly seen in the plot as a discontinuity in the

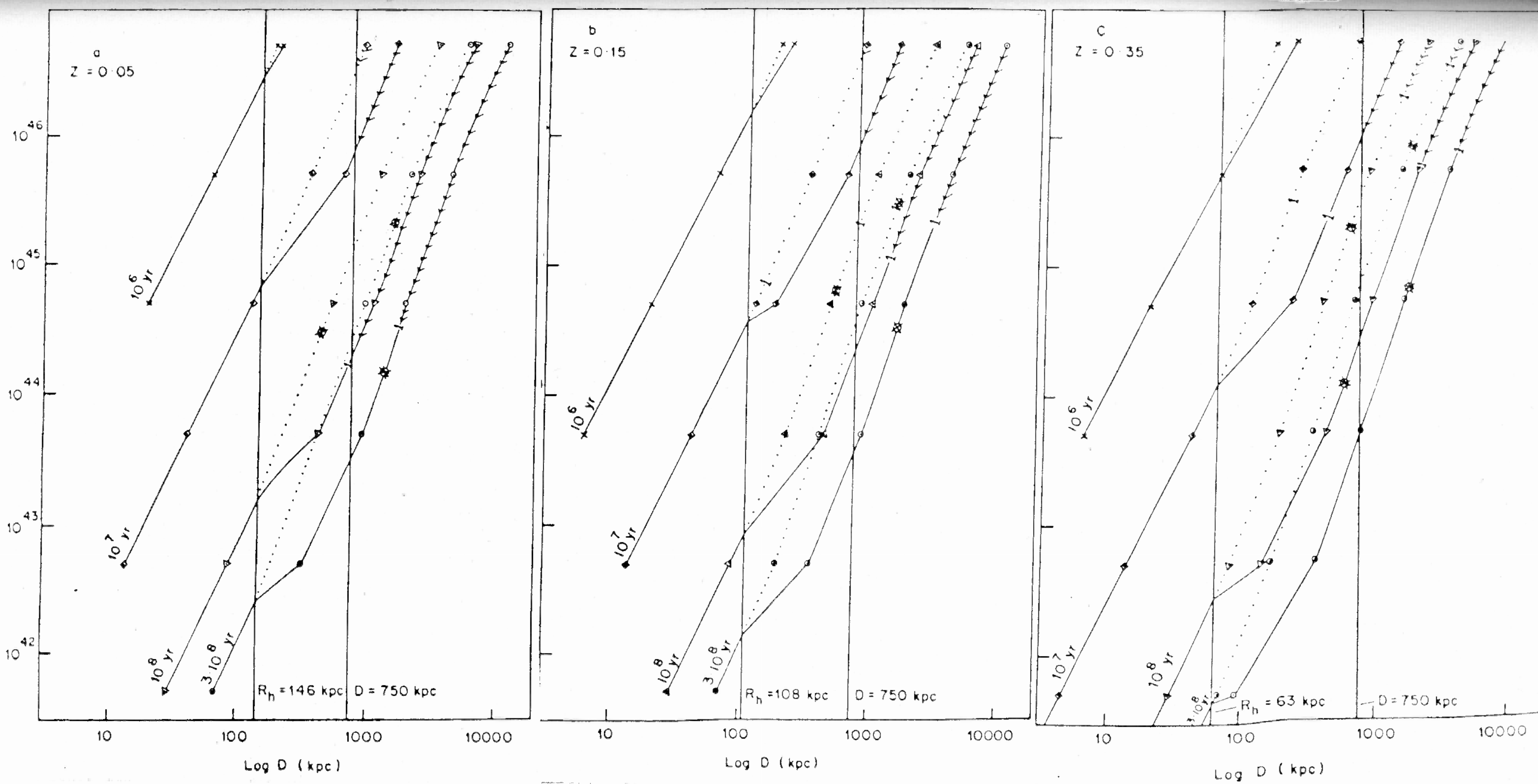

Fig.6.1a-c The dependence of size (D) on the beam power (L_b) at four different ages, for three redshifts in Model A (continuous lines) and Model B (dotted lines). The different symbols represent, ✱ : When the beam becomes subsonic; and 1: when $S_{1\ GHz}$ = 1 Jy. The ticked lines indicate evolution of GRGs free of constraints. The vertical lines represent the galaxy halo radius (R_h) and the minimum GRG half-size of 750 kpc. The redshift is indicated on the top left hand corner.

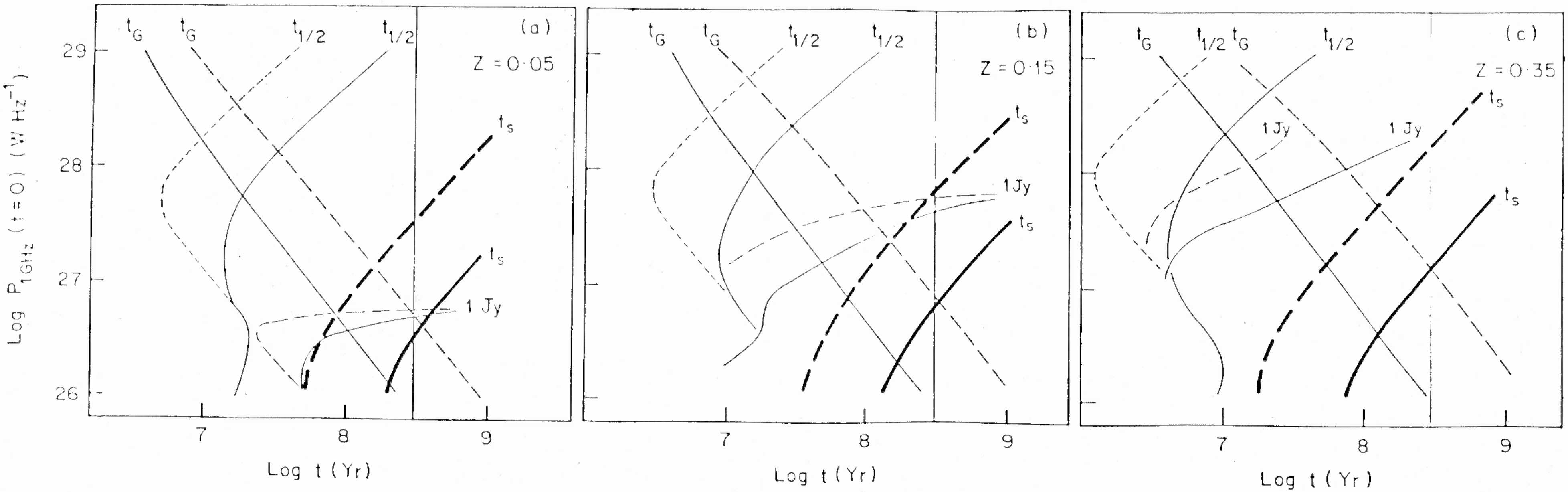

Fig.6.2a-c Dependence of several important timescales on the initial radiated power, P_o, at 1 GHz, is shown for three redshifts in Model A (continuous lines) and Model B (dashed lines). The various symbols represent : $t_{1/2}$, the time at which the radio power falls to half its initial values; t_G, the time at which the source becomes a GRG; t_s, the time at which the motion of the beam's head becomes sonic; and $t_{1\ Jy}$, the time at which the flux falls to the detection limit of 1 Jy at 1 GHz.

Table 6.1 a

Minimum total beam power (both beams included) to form a GRG observable above the level of S_{1GHz} = 1Jy within the lifetime $t_N = 3.10^8$ yr for different z for Model A and Model B

z	$2L_b$(erg s^{-1})	
	Model A	Model B
0.05	$6.6.10^{44}$	–
0.15	$4.5.10^{45}$	$5.7.10^{45}$
0.15	$1.55.10^{46}$	$6.6.10^{46}$

Table 6.1 b

Maximum size (kpc) attained within the lifetime $t_N = 3.10^8$ yr having $S_{Lim} >$ 1 Jy at different z and beam power for Model A / Model B.

z	$2L_b$(erg s^{-1})		
	10^{45}	10^{46}	10^{47}
0.05	1950/930	4400/2110	$1.2.10^4$/5817
0.15	-/-	4100/1900	$1.02.10^4$/5200
0.35	-/-	-/-	8000/4200

Table 6.2. The model predictions for average radio luminosities and the numbers of giant radio sources ($H_o = 50$ kms^{-1} Mpc^{-1}, $q_o = 0$) S_{lim}=1.0 Jy at 1 GHz.

		Model A						Model B						Model AB			
		$t_N = 10^8$ yr			$t_N = 3.10^8$ yr			$t_N = 10^8$ yr			$t_N = 3.10^8$ yr			$t_N = 10^8$ yr		$t_N = 3.10^8$ yr	
z-range	ΔV	Log P_o^*	N	Log<P>	Log P_o^*	N	Log<P>	Log P_o^*	N	Log<P>	Log P_o^*	N	Log<P>	N	Log<P>	N	Log<P>
	Gpc^3	W/Hz		W/Hz	W/Hz		W/Hz	W/Hz		W/Hz	W/Hz		W/Hz		W/Hz		W/Hz
0.0-0.1	0.79	26.75	11	26.2	26.75	72	26	27.5	0.6	26.4	27.25	10	26.6	2.6	26.3	27	26.3
0.1-0.2	4.74	27.25	25	26.6	27.25	41	26.8	27.75	4.4	26.3	27.75	35	26.3	10	26.5	38	26.6
0.2-0.3	11.1	27.5	24	27.1	27.5	31	27.3	28.25	2	27	28.25	7.9	27.4	6.6	27.03	16	27.3
0.3-0.4	18.7	27.75	17	27.4	27.75	20	27.5	28.5	1	27.2	28.5	3.8	27.2	4	27.3	9	27.4
0.4-0.5	27.0	28	13	27.5	28.0	13.5	27.5	28.5	0.04	27.1	28.5	0.04	-	0.7	27.3	1	-
0.5-0.6	35.9	28.25	11	27.8	28.25	12	27.9	29									
Total (z = 0-0.6)	98.2		101			190			8			57		24		91	

Notes : Model AB is the geometetric mean of Models A and B. P_o^* is the minimum initial radio luminosity needed to produce a GRG (2D = 1.5 Mpc) observable above the flux density limit at 1 GHz of 1Jy. N is the number of observable GRG's limited either by the flux threshold or the nuclear life time. <P> is the mean radiated power at 1 GHz for GRG's at typical overall size of 2D = 2 Mpc different curves pertaining to Model A. In Table 6.1 we list the values of the minimum total beam powers ($2L_b$) required to produce an observable GRG (S_{Lim} > 1 Jy) within the lifetime of the central engine $t_N = 3.10^8$ yr for redshifts of 0.05, 0.15 and 0.35, as read from Fig.6.1. Also from Fig.6.1, we get the values of the maximum observable size attained for different beam powers, within the lifetime of the central engine for different z, which are tabulated in Table 6.1. The formation of an observable GRG is understandably more difficult in case of Model B which assumes a continuity in the head velocity across the interface, making the beam flare and actually decelerate within the tenuous IGM. Also at higher redshifts, more energetic beams are required. From Table 6.1, it is seen that for a given total beam power the maximum observable size attained reduces with increasing redshift, indicating the cosmological evolution of linear size.

In Fig.6.2, we illustrate the dependence of various timescales important in the evolution of the radio galaxy, on the initial radio power P(0) for different values of redshift. P(0) is taken as a fraction (ϵ = 0.1), of the beam power. In these plots, the region bounded by the lines representing t_{GRG}- the time at which a source of a given initial radio power becomes a GRG, the line drawn at $t = t_N = 3.10^8$ yr, and t_{1Jy}-the time when the radio output becomes 1 Jy at 1 GHz is the region of interest. Here the source spends part of its life as a GRG. A feature that can be clearly noted from the 3 plots is, the shrinking of this region, with increasing redshift. At higher redshifts, only high radio power sources can form, and be detected as GRGs.

In estimating the total numbers of observable GRGs distributed over the whole sky, we need to use our estimates of the time spent as an observable GRG which is a function of beam power and redshift, along with the appropriately transformed radio luminosity function (RLF) at various redshifts (see below). For this we used the RLF for steep spectrum sources given in Fig.2 of Peacock (1987), and converted the values appropriate to $q_0 = 0$ (consistent with our definition of a GRG) using relations given in Peacock (1987).

Since, for our exercise we require a knowledge of the number density of sources as a function of total beam power, rather than the observed radio power, we need to convert the RLF to a beam power function. For this we should use the relation between the radio power and beam power. But as this varies during the evolution of the source (due to setting in of RRE; see Section 6.3) the conversion becomes somewhat imprecise.

We find from the model (Fig.1 in Gopal-Krishna and Wiita, 1988) that Log P remains nearly constant at approximately Log (ϵ $2L_b$) until a time $t_{1/2}$ when it has decreased by 0.3. After that the decay is quite abrupt due to RRE. Hence, to a first approximation, P may be regarded as constant for t

$\leq$ $t_{1/2}$ and effectively zero thereafter. Thus, to this approximation, sources now observed at a given power P must have turned on essentially at that power during the past $t_{1/2}$ years. A few sources of higher initial powers that turned on at even earlier times would also now be observed at P, but it is impossible to isolate them from the existing data; their numbers must, however, be small in view of the steepness of the RLF. Because of this unavoidable omission, the values for the numbers of GRGs given below (Table 6.2) are somewhat overestimated.

The rate of creation of sources per unit volume with a total beam power $2L_b$ ($\approx L_R(0)/\epsilon \approx 10^{10} P(0)/\epsilon$) is approximately equal to the observed number density of sources with power P divided by $t_{1/2}$ for that value of P (The same procedure must be carried out for each redshift interval). Further, a source would be observed as a GRG only provided the time t_G, it takes to grow to 2D=1.5 Mpc is shorter than the time $t_\star$ over which it would remain observable after its creation, subject to one or the other set of constraints involving t_N and S_{Lim}. If we define $P^\star$ as the minimum initially radiated power required to produce a GRG using a particular set of constraints, the number of observable GRGs in a given redshift bin is equal to

$$N(z)\Delta z = \Delta V(z) \int_{P^\star}^{\infty} [t_\star(P,z) - t_G(P,z)] \frac{\rho(P,z)}{t_{1/2}(P,z)} dP \Delta z. \qquad ...(6.13)$$

with Δ V(z) being the volume contained within z-z/2 and

$z+z/2$, and the integral being defined only for non-negative values of the quantities within the square brackets. The function $V(z)$ for $q_o = 0$ is obtained by differentiating the following expression (e.g., Windhorst, 1984):

$$V(<z) = 4\pi \left(\frac{c}{H_o}\right)^3 \left[\frac{1}{8} \left\{ (1+z)^2 - \frac{1}{(1+z)^2} \right\} - \frac{1}{2} \ln (1+z) \right] \qquad \ldots(6.14)$$

Table 6.2 gives the values of ΔV, P^* and N for 6 redshift intervals upto $z = 0.6$, for Model A, Model B and a composite Model AB, for the detection limit of $S_{1GHz} = 1$ Jy and two values of limiting nuclear lifetimes of $t_N = 10^8$ yr and 3.10^8 yr. Since the RLF is poorly defined at $z \geq 0.6$ for the very high powers needed to form GRGs at such redshifts, the applicability of this analysis is restricted to lower redshifts. Since Models A and B represent opposite extremes of the behaviour of a beam crossing the interface (Section 6.2), leading to over- and under-estimates of GRGs, respectively, we have also tabulated geometrical means of N under the heading 'Model AB'. The composite model should be closer to reality than either Model A or Model B (see RW).

As expected, the minimum initial radio power, P^*, required to form a GRG increases with z, and because the RLF falls steeply with P, fewer GRGs would be predicted at higher z. On the other hand, the volume elements $\Delta V(z)$ are larger, and, moreover, the RLF increases due to the cosmological evolution as one goes to higher z. These countervailing trends produce the different runs of N with z seen in Table 6.2.

To predict the mean radio luminosity <P> of GRGs as a function of redshift, we consider the radio power, P_{1Mpc}, at the value D = 1 Mpc which is the typical half-size of the known GRGs (Saripalli et al., 1986). Thus we obtain

$$< P(z) > = \frac{\Delta V(z)}{N(z)} \int_{P^*}^{\infty} P_{1Mpc}(P,z)[t_*(P,z) - t_G(P,z)] \frac{\rho(P,z)}{t_{1/2}(P,z)} dP \quad ...(6.1)$$

where N(z) is given by Eq.(6.13). The predicted values of <P> at 1 GHz are given in Table 6.2 for Models A,B and AB.

6.5 DISCUSSION

We have studied the evolution of the giant radio galaxies using the beam propagation model of Gopal-Krishna and Wiita (1987), incorporating losses incurred due to inverse Compton scattering of the relativistic electrons in the lobes against the microwave background and relativistic motion of the beam's head. We have employed an observational constraint of a detection limit of S_{1GHz} = 1 Jy at 1 GHz, and upper bounds to the nuclear life time of 10^8 and 3.10^8 yr, to the powers and numbers (over entire sky) of observable GRGs as a function of redshift. From Table 6.2, it is seen that the predicted mean radio luminosities at 1 GHz (for the composite model AB) for $t_N = 10^8$ yr and 3.10^8 yr and redshift z < 0.1 are both $10^{26.3}$ WHz^{-1}. This agrees very well with the mean $10^{25.9}$ WHz^{-1} found for the 9 GRGs at z < 0.1 (Saripalli et al. 1986; Table 2.5). At higher redshifts the predicted powers are higher, in agreement with the scanty data available for the GRGs at z>0.1. The mean powers are seen to increase slowly with redshift.

For comparing the predicted number of observable GRGs over the whole sky with that inferred from existing data, we use the published results of the 6C survey (Baldwin et al., 1985). With a combination of low observing frequency, (151 MHz), a resolution of 4'.4 x 4'.4 cosec δ, a high sensitivity of 200 mJy/beam (5 rms) and a large sky coverage ($\sim$ 3 steradian), the 6C survey is well suited for picking out GRGs. For z<0.1, a source would require a minimum size of $\sim$ 10 arc to be a GRG by our definition. In this exercise we have predicted the total number of GRGs having z<0.1, and having $S_{1\ GHz}$>1Jy above which the 6C survey (for GRGs) is unaffected by confusion*. Such sources would therefore have been well resolved and recognized as GRGs. We would therefore be fairly justified in assuming a high degree of completeness in the detection of such sources in the whole of the 6C sample. There are 7 known GRGs ($\delta > 30^{\circ}$) meeting these criteria which extrapolates to $\sim$ 30 GRGs over the whole sky. Our prediction of 25 - 30 GRGs for the composite model AB with $t_N = 3.10^8$ yr and z<0.1 agrees remarkably well with the $\sim$ 30 GRGs estimated for the whole sky. This good agreement lends confidence in the prediction of 91 observable GRGs over the entire sky and all redshifts, for the same set of constraints. At higher redshifts (z > 0.1) we predict a larger number of GRGs which, however have not been found so far. Over the whole sky only 5 GRGs are known having z > 0.1. Possible causes of this discrepancy are likely to be related to observational difficulties:

*extrapolating from $S_{151MHz} \simeq 5$ Jy, given by Saunders et al. (1987)

1. For such (distant) sources, the low surface brightness extensions (or bridges) will be more difficult to detect, thereby causing the GRG to be misidentified as two unrelated sources.
2. The parent galaxy will not so readily stand out due to its faintness.
3. The recognition of sources as GRGs at higher redshifts would be clearly hampered by the lack of sufficient angular resolution. Due to this, the faint radio extensions from the hotspots towards each other, a crucial hint for physical association, may appear merged with the hotspots. The source would therefore be confused as two unrelated sources.

The third difficulty has clearly been shown to be the case by Saunders et al., (1987), who observed 9 6C fields containing suspected GRGs with higher resolution. With the higher resolution follow-up, they could confirm as many as 4 sources as large doubles with size exceeding a megaparsec (having redshifts $z>0.1$) and 3 others with a high probability of having megaparsec sizes. Their results clearly indicate the existence of a large number of potential, (distant) GRGs in the 6C catalogue,consistent with our prediction (Table 6.2). A systematic observational effort in this direction is clearly needed.

6.6 CONCLUSIONS

Through reasonable assumptions concerning the properties of jets, galactic haloes and the IGM, and using the analytic model of Gopal-Krishna and Wiita(1987;1988) for the beam propagation we have been able to predict the numbers and mean radio powers of GRGs which agree remarkably well with the observations. The main conclusions of this work (see also Gopal-Krishna, Wiita and Saripalli, 1988) is that giant radio sources are produced by intrinsically powerful AGNs whose radio luminosities suffer declines of nearly an order-of-magnitude between the point of their turning-on and their becoming GRGs. An indication of this also comes from the statistically high prominence of their radio cores, which is comparable to the intrinsic prominence of the cores of radio-loud quasars (Saripalli et al., 1986). Our results are based on the assumption that the beams are relativistic throughout their lengths, which is supported, a posteriori, by the consistency with the observations. The model predicts that a systematic, high resolution follow-up of GRG candidates picked from a 6C type survey would lead to the discovery of a large number of GRGs at moderately high redshifts, where very few GRGs have been found so far.

Future Work:

Although the results presented here are in good agreement with the available data, we have so far considered only fixed values of parameters that appear most reasonable. Parameters such as ϵ, the initial ratio of the radio to beam power; η , the ratio of the average magnetic energy density of the entire source to that of the hot spots; and even a, δ and T, the scale-height, power-law index, and temperature of the gaseous halo, are expected to have significant dispersions, and ranges of such parameters will be explored in future work.